# Assessment and comparison of several analytical models of water impact

**Alan Tassin[1,2], Nicolas Jacques[1], Aboulghit El Malki Alaoui[1], Alain Nême[1], Bruno Leblé[2]**

[1]Laboratoire Brestois de Mécanique et des Systèmes (EA 4325 LBMS), ENSIETA/Université Européenne de Bretagne, 2 rue François Verny, 29806 Brest cedex 9, France

[2]DCNS - Ing. Navire Armé, DCSE/CSB, rue Choiseul, 56311 Lorient Cedex, France

E-mail adresses: alan.tassin@ensieta.fr; nicolas.jacques@ensieta.fr; aboulghit.elmalkialaoui@ensieta.fr; alain.neme@ensieta.fr; bruno.leble@dcnsgroup.com

**ABSTRACT**

This paper deals with the accuracy of several analytical models for the prediction of the hydrodynamic force and pressure distribution acting on a body entering initially calm water. The problem of water entry is important for the analysis of slamming loads undergone by boats operating in waves, as well as of the steady behaviour of high-speed planing vessels. The considered models are briefly described and the obtained results are compared to those of numerical computations and experimental observations for a number of two-dimensional and axisymmetric cases of water impact.

**Keywords:** water impact, slamming, Wagner theory.

## 1. INTRODUCTION

The design of naval and offshore structures includes the consideration of water impact related loads. An example of water impact problem is the slamming of a ship's bow in heavy sea conditions. Slamming loads can induce important transient stresses and affect the integrity of local structural components. Slamming also causes global effects on ship structures such as whipping, a transient vibration of the ship that may cause significant fatigue damage [1–2].

It is now possible to solve complex hydrodynamic impact problems using Computational Fluid Dynamics (CFD) techniques [3–6]. Nevertheless, CFD methods require large computational resources, which prohibits their use for preliminary design. As a result, analytical models of water impact are still useful tools for engineering applications. Pioneering work on the subject was performed by von Karman [7], who was concerned with seaplane landing problems. The model of von Karman was subsequently refined by Wagner [8] by taking into account the local uprise of the water to determine the wetted surface (contact surface between the impacting body and the fluid). The Wagner model was originally restricted to two-dimensional problems and was afterwards extended to axisymmetric cases by Chuang [9]. Recently, Scolan and Korobkin [10] have used the Wagner method to study the impact of three-dimensional bodies. The Wagner theory is based on the so-called "flat disc assumption". This means that the boundary conditions are linearized and imposed on the initially flat liquid free surface. It is obvious that this assumption is only valid for an impacting body with small deadrise angle (angle between the

tangent to the body profile and the initial free surface). Besides, the Wagner theory predicts an infinite pressure at the intersection between the surface of the impacting body and the liquid free surface. The singularity is integrable (when the pressure is computed with a linearized form of the Bernoulli equation) and the hydrodynamic force acting on the impacting body can be determined. Nevertheless, it has been observed that the Wagner theory overpredicts the impact loads [2, 11]. Several pieces of work have been done to develop more accurate simplified models of water impact. Some models were obtained using the method of matched asymptotic expansions in which the jet flow occurring in the vicinity of the intersection between the free surface and the body is taken into account [12, 13]. The extension of this method to three-dimensional problems has been discussed by Scolan and Korobkin [14]. Other semi-analytical models are based on the generalized Wagner theory [15–18]. In this case, only the boundary condition on the free surface is linearized, the body boundary condition being imposed on the actual position of the body. It should be noted that the models based on the generalized Wagner approach are much more complex than Wagner models and, for arbitrary sections, the instantaneous flow around the body must be computed numerically. In addition, to our knowledge, axisymmetric generalized Wagner models are not available. The models proposed by Korobkin [11] are based on Wagner's flat-disc approximation, but the shape of the impacting body and the nonlinear term of the Bernoulli equation are taken into account in an approximate way.

The present work is dedicated to the assessment and comparison of several models of water impact. Contrary to previous work on the subject [12, 19], the present study is not restricted to two-dimensional bodies having a simple geometry. Three analytical models have been considered: the model of Zhao and Faltinsen [13], which is based on the matched asymptotic expansions method, the modified Logvinovich model and a simplified generalized Wagner model, which have been proposed by Korobkin [11]. These models are based on the flat disk assumption. They are therefore easy to implement and can be used as engineering tools. Besides, they can be applied to both two-dimensional and axisymmetric problems. The accuracy of the three models is investigated through comparisons with results of finite elements computations and with experimental data.

## 2. THE WAGNER THEORY OF WATER IMPACT

### 2.1. BASIC ASSUMPTIONS

The problem of a two-dimensional symmetric body or an axisymmetric body penetrating vertically into an unbounded liquid domain initially at rest is considered. The body is assumed to be rigid and its velocity to be constant in the present study. It is assumed that the liquid's inertia dominates the forces acting on the body during the typical duration of the impact. The effects of viscosity, surface tension, compressibility, gravity and air-cushion are neglected. The flow is assumed to be irrotational.

Wagner supposed that, during the initial stage of impact of a blunt body, the deadrise angle remains small and that the liquid surface is close to its initial position. Consequently, the instantaneous fluid flow is more or less the same as if the fluid was loaded by a flat plate. Thus, within the Wagner approach, the body surface boundary condition is imposed on the initial flat position of the liquid free surface (Figure 1). The free surface boundary is also simplified by considering a linearized form of the Bernoulli equation:

$$p = -\rho \partial \varphi / \partial t, \tag{1}$$

where $\rho$ is the fluid density, $p$ is the hydrodynamic pressure and $\varphi$ is the velocity potential. Therefore, under Wagner's assumptions, the velocity potential satisfies the following set of equations:

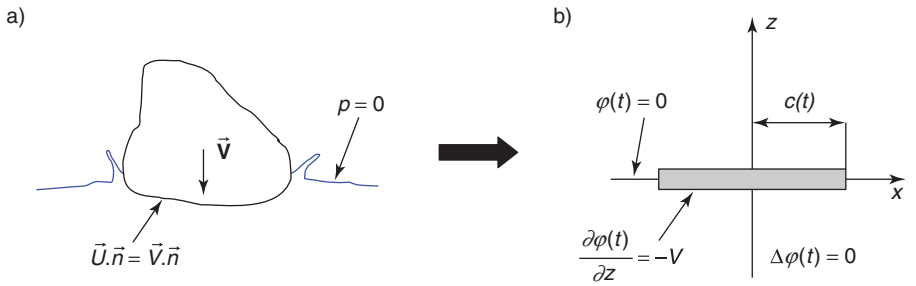


Figure 1 Sketches of the water entry problem (a) and its approximation within the Wagner theory (b).

$$\begin{cases} \Delta\varphi = 0 & \\ \varphi = 0 & z = 0,\ |x| > c(t) \\ \dfrac{\partial\varphi}{\partial z} = -V & z = 0,\ |x| < c(t)\ . \\ \varphi \to 0 & \sqrt{x^2 + z^2} \to \infty \end{cases} \tag{2}$$

where $V$ is the velocity of the impacting body and $c$ is the half-length of the contact region. The solution of this boundary-value problem is well-known for both the two-dimensional (2D) [2, 8] and axisymmetric (axi.) [10] cases. The velocity potential in the contact region ($|x| < c(t)$) can be written in the following form:

$$\begin{cases} \varphi = -V\sqrt{c(t)^2 - x^2}, \text{ 2D} \\ \varphi = -2V\sqrt{c(t)^2 - x^2}/\pi, \text{ axi.} \end{cases} \tag{3}$$

At this stage, the wetted surface width $c(t)$ is unknown and has to be determined.

## 2.2. DETERMINATION OF THE WETTED SURFACE

The half-length of the wetted surface $c(t)$ corresponds to the abscissa of the point of intersection between the body surface and the water free surface (Figure 2). It is therefore necessary to compute the elevation of the free surface to determine $c(t)$. The analytical

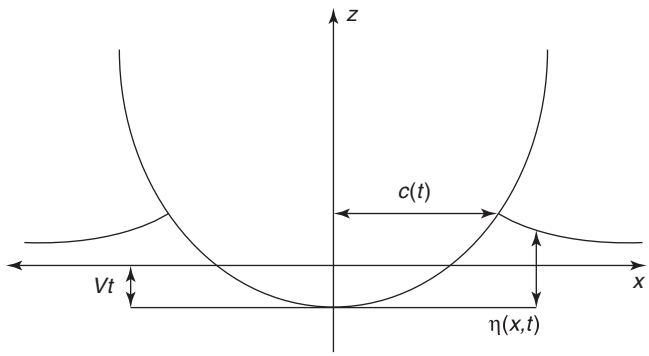


Figure 2 Definition of geometric parameters.

solution for the velocity potential makes it possible to express the relative vertical velocity $U_r$ between a point on the free surface and the body (for $|x| > c(t)$) as:

$$\begin{cases} U_r(x,t) = \dfrac{\partial \varphi}{\partial z} + V = \dfrac{V|x|}{\sqrt{x^2 - c(t)^2}}\ , \text{2D} \\ U_r(x,t) = \dfrac{\partial \varphi}{\partial z} + V = \dfrac{-2V}{\pi}\left[\arcsin\left(\dfrac{c(t)}{x}\right) - \dfrac{c(t)}{\sqrt{x^2 - c(t)^2}}\right] + V, \text{ axi.} \end{cases} \tag{4}$$

As mentioned above, within the Wagner approach, the free surface condition is $\varphi = 0$. Consequently, the horizontal velocity is zero on the free surface. Thus, the relative elevation of the free surface $\eta(x, t)$ can be obtained by the time integration of the relative velocity $U_r$:

$$\eta(x, t) = \int_0^t U_r(x, \tau)\, d\tau \quad . \tag{5}$$

At the intersection between the body surface and the free surface, the relative elevation $\eta$ is equal to the initial position of the body shape (Figure 2):

$$f(c(t)) = \eta(c(t), t). \tag{6}$$

where function $f$ describes the body shape. Eqn. (6) is often referred to as the Wagner condition and makes it possible to find the wetted surface as a function of time. However, a closed-form solution for $c(t)$ can only be derived for simple shapes (wedge, parabola, cone and axisymmetric paraboloid). For arbitrary sections, the Wagner condition must be solved numerically. The method used in the present work is presented in Appendix.

## 3. MODELS FOR THE PRESSURE DISTRIBUTION

This section presents several analytical models for the prediction of the hydrodynamic pressure distribution on the impacting body. These models are based on the velocity potential provided by the Wagner theory.

### 3.1. ORIGINAL WAGNER MODEL [8]

By considering the Bernoulli equation,

$$p = -\rho \frac{\partial \varphi}{\partial t} - \frac{1}{2}\rho(\nabla \varphi)^2\ , \tag{7}$$

and the velocity potential in the contact region, Eqn. (3), the distribution of pressure acting on a solid entering a liquid at constant velocity can be written in the following form:

$$\begin{cases} p(x) = \dfrac{\rho V c}{\sqrt{c^2 - x^2}}\dfrac{dc}{dt} - \dfrac{\rho V^2 c^2}{2(c^2 - x^2)}, \text{2D} \\ p(x) = \dfrac{2\rho V c}{\pi\sqrt{c^2 - x^2}}\dfrac{dc}{dt} - \dfrac{2\rho V^2 x^2}{\pi^2(c^2 - x^2)} - \dfrac{\rho V^2}{2}, \text{ axi}. \end{cases} \tag{8}$$

It should be noticed that the pressure is negative and infinite at $|x| = c(t)$. Moreover, the singularity is not integrable. Wagner indicated that Eqn. (8) is expected to provide an accurate estimation of the pressure only near the centre of the contact region. In this region, the second term of the right-hand side of Eqn. (8) is much smaller than the first term. Thus, Wagner suggested that this term (which corresponds to the quadratic term of the Bernoulli equation) should be disregarded when calculating the total hydrodynamic force acting on the body. In other words, Wagner suggested that the hydrodynamic pressure should be computed using the linearized Bernoulli, Eqn. (1). This gives:

$$\begin{cases} p(x) = \dfrac{\rho V c}{\sqrt{c^2 - x^2}} \dfrac{dc}{dt}, \text{ 2D} \\ p(x) = \dfrac{2\rho V c}{\pi\sqrt{c^2 - x^2}} \dfrac{dc}{dt}, \text{ axi}. \end{cases} \tag{9}$$

In this case, the pressure remains positive on the whole body surface but is still infinite at $|x| = c(t)$. However, the singularity is integrable.

### 3.2. ZHAO AND FALTINSEN MODEL [13]

The infinite pressure predicted by the original Wagner model is of course unphysical and Wagner indicated that a detailed analysis of the jet flow occurring near the intersection between the body and the free surface is required to obtain the correct pressure near $|x| = c(t)$. This analysis was already performed by Wagner. However, Wagner did not known how to match the local jet flow solution and the one obtained from the flat plate approximation. This problem was overcome for the first time by Cointe and Armand [12] using the method of matched asymptotic expansions. Thanks to this technique, a composite pressure distribution valid on the whole contact area was obtained.

The Zhao and Faltinsen model (ZFM) [13] is also based on the method of matched asymptotic expansions. For $|x| < c(t)$, the pressure distribution is of the form:

$$\begin{cases} p(x) = \dfrac{\rho V c}{\sqrt{c^2 - x^2}} \dfrac{dc}{dt} - \dfrac{\rho V c}{\sqrt{2c(c-x)}} \dfrac{dc}{dt} + 2\rho \left(\dfrac{dc}{dt}\right)^2 \dfrac{\sqrt{\tau}}{\left(1+\sqrt{\tau}\right)^2}, \text{ 2D} \\ p(x) = \dfrac{2\rho V c}{\pi\sqrt{c^2 - x^2}} \dfrac{dc}{dt} - \dfrac{2\rho V c}{\pi\sqrt{2c(c-x)}} \dfrac{dc}{dt} + 2\rho \left(\dfrac{dc}{dt}\right)^2 \dfrac{\sqrt{\tau}}{\left(1+\sqrt{\tau}\right)^2}, \text{ axi.} \end{cases} \tag{10}$$

For $x \geq c(t)$, the pressure is related to the jet flow solution:

$$p(x) = 2\rho\left(\frac{dc}{dt}\right)^2 \frac{\sqrt{\tau}}{\left(1+\sqrt{\tau}\right)^2}. \tag{11}$$

$\tau$ is a positive number that is solution of the following equation:

$$x - c = (\delta/\pi)(-\ln\tau - 4\sqrt{\tau} - \tau + 5), \tag{12}$$

where $\delta$ is the thickness of the jet:

$$\begin{cases} \delta = \pi V^2 2c/[4dc/dt]^2, \text{2D} \\ \delta = V^2 c/\left(2\pi[dc/dt]^2\right), \text{axi.} \end{cases} \tag{13}$$

It should be noted that the original model of Zhao and Faltinsen [13] was dedicated to two-dimensional problems. Its extension to axisymmetric problems was proposed by Scolan [20].

### 3.3. MODIFIED LOGVINOVITCH MODEL AND SIMPLIFIED GENERALIZED WAGNER MODEL OF KOROBKIN [11]

Korobkin generalized Wagner's ideas in a different way. In his work, Korobkin analysed several models of water impact including the generalized Wagner model [15], the Vorus model [21] and the Logvinovich model. He suggested that better predictions of the hydrodynamic pressure could be achieved by taking into account nonlinear effects related to the quadratic term of the Bernoulli equation and to the real geometry of the wetted surface. From this analysis, he derived two new models of water impact.

The distributions of pressure $P(x, t)$ and of velocity potential $\phi(x, t)$ on the wetted surface are defined by:

$$P(x, t) = p(x, f(x) - h(t), t), \tag{14}$$

$$\phi(x, t) = \varphi(x, f(x) - h(t), t), \tag{15}$$

where $h(t)$ is the penetration depth of the impacting body $h(t) = Vt$ and function $f$ describes the body shape. $\varphi$ is the velocity potential corresponding to the exact water impact problem (with no linearization of the boundary conditions). By using the body surface boundary condition:

$$\varphi_{,z} = \varphi_{,x} f_{,x} - V, \tag{16}$$

the pressure distribution can be written in the following form:

$$P(x, t) = -\rho \left[ \phi_{,t} + \frac{f_{,x} V}{1 + f_{,x}^2} \phi_{,x} + \frac{1}{2} \frac{\phi_{,x}^2 - V^2}{1 + f_{,x}^2} \right]. \tag{17}$$

It should be pointed out that this expression is only based on the assumption that the flow is potential. However, the computation of the pressure $P(x, t)$ requires the velocity potential $\varphi(x, z, t)$, which can only be determined using numerical methods. To overcome this difficulty, it was proposed that $\varphi(x, z, t)$ should be approximated with the use of the velocity potential $\varphi^{(w)}$ obtained from the classical Wagner theory:

$$\varphi(x, z, t) \approx \varphi^{(w)}(x, z - d(t), t), \tag{18}$$

where $d(t)$ is the $z$-coordinate of the plane on which the boundary conditions are projected in the Wagner theory. Moreover, the wetted surface is computed according to the Wagner theory, see section 2.2. Then, a first order Taylor expansion of $\varphi^{(w)}$ around $z = d(t)$ is used to simplify the computation of $\phi(x, t)$.

In the Modified Logvinovich Model (MLM), the linearization of the water entry problem is performed around the initial liquid level, $d(t) = 0$, leading to the following expression:

$$\phi(x, t) \approx \varphi^{(w)}(x, 0, t) - V[f(x) - h(t)], \tag{19}$$

In the Generalized Wagner Model (GWM), the linearization is performed around a flat surface at the height of the intersection between the body and the free surface, $d(t) = f(c(t)) - h(t)$, leading to the following expression:

$$\phi(x, t) \approx \varphi^{(w)}(x,0,t) - V[f(x) - f(c(t))]. \tag{20}$$

The pressure distributions are then obtained by inserting Eqn. (19) and Eqn. (20) into Eqn. (17).

## 4. NUMERICAL SIMULATIONS

For comparison purposes, numerical simulations of water impact have been performed with the finite element software ABAQUS/Explicit. For these simulations, water is modelled as a compressible viscous fluid:

$$\underline{\underline{\sigma}} = -p\underline{\underline{I}} + 2\mu\underline{\underline{D}}', \quad \text{with} \quad p = K\left(1 - \frac{V}{V_0}\right), \tag{21}$$

where $\underline{\underline{\sigma}}$ is the Cauchy stress tensor and $\underline{\underline{D}}'$ is the deviatoric part of the strain rate tensor. $K$ and $\mu$ are respectively the bulk modulus and the viscosity (in this analysis, $K = 2.03 \times 10^9$ Pa, $\mu = 0.001$ Pa.s).

Water impact problems involve high velocity flows and cannot be treated effectively with Lagrangian methods. Thus, for the present simulations, the Arbitrary Lagrangian Eulerian (ALE) formulation of the ABAQUS software has been used. ALE formulations combine the features of Lagrangian and Eulerian analyses and make it possible to overcome the difficulties due to mesh distortion. The ALE technique of ABAQUS is based on the operator splitting method. This means that each analysis increment consists of a Lagrangian phase (in which the mesh moves with the fluid flow) followed by an advection phase. During the latter stage, the following tasks are performed: First, a new mesh is created in order to reduce mesh distortion. Then, the element state variables (stress and density) and the nodal velocities are transferred from the old mesh to the new mesh.

The fluid mesh consists of two areas. The first one is located near the impact surface where the fluid undergoes a large amount of deformation. In this area, a fine ALE mesh of 4-node quadrilateral elements (ABAQUS CPE4R for two-dimensional problems and CAX4R for axisymmetric problems) is used; the mesh size is about 150 $\mu$m. Out of this area, the deformation of the fluid remains moderate. Therefore, a Lagrangian mesh of linear triangular elements is used (Figure 3). The size of the fluid domain has been chosen in order to avoid any effect of the boundary conditions at its exterior surface. Indeed, in the present computations, the fluid compressibility is taken into account. Therefore, the impact generates acoustic waves, which reflect back as it reaches the boundary of the fluid domain. To prevent any interaction between the impacting body and the reflected waves, the following condition should be fulfilled:

$$L \geq \frac{c_0 T}{2}, \tag{22}$$

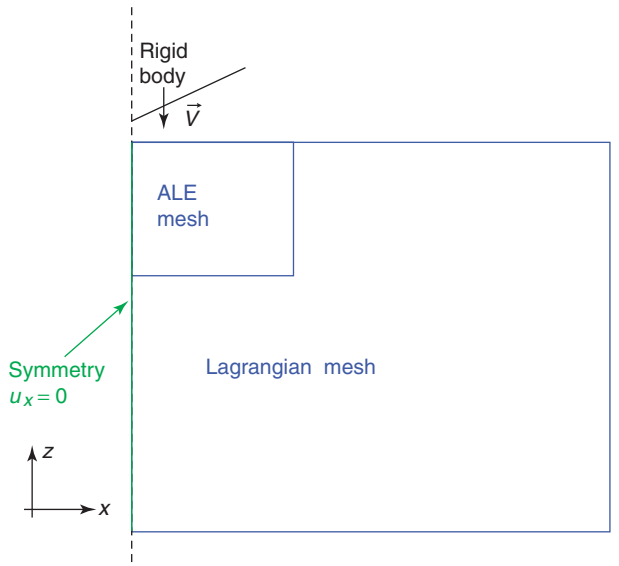


Figure 3 Sketch of the finite element model.

where $L$ is the distance between the impact area and the exterior surface of the fluid domain, $T$ is the time period simulated and $c_0$ is the speed of sound $(c_0 = \sqrt{K/\rho})$.
The impacting solid is modelled as a rigid body. Frictionless contact is used to describe the interaction between the fluid and the impacting body.

## 5. RESULTS

In this section, several test cases are presented. The results derived from the analytical models are compared with those of the finite element simulations and with experimental data.

### 5.1. WEDGES AND CONES

Figure 4 displays distributions of pressure coefficient $Cp$ along the surface of a wedge entering water at constant velocity for several values of the deadrise angle. The pressure coefficient is defined as:

$$Cp = 2P/(\rho V^2). \tag{23}$$

For the smallest deadrise angle (Figure 4.a), the pressure distributions predicted by the analytical models are in close agreement with the numerical results. As the deadrise angle increases, more pronounced discrepancies are observed (Figure 4.b and Figure 4.c). Even if the MLM and the GWM overestimate the peak pressure, they seem to be more accurate than the ZFM. Figure 5 compares the nondimensional force on a wedge as a function of the deadrise angle. In addition to the results obtained with ZFM, MLM, GWM and ABAQUS, the slamming forces provided by the original Wagner theory and the similarity solution are also displayed. The similarity solution results were obtained by Zhao and Faltinsen [13] using the analytical formulation proposed by Dobrovol'skaya [22]. The similarity solution does not require any assumption concerning the shape of the liquid surface. Therefore, it is often considered as a reference solution for the problem of wedge entry into an incompressible ideal fluid. It is, however, not an exact solution since it is implicitly given in terms of integral equations, which must be solved numerically. One observes that the similarity solution is very closed to the

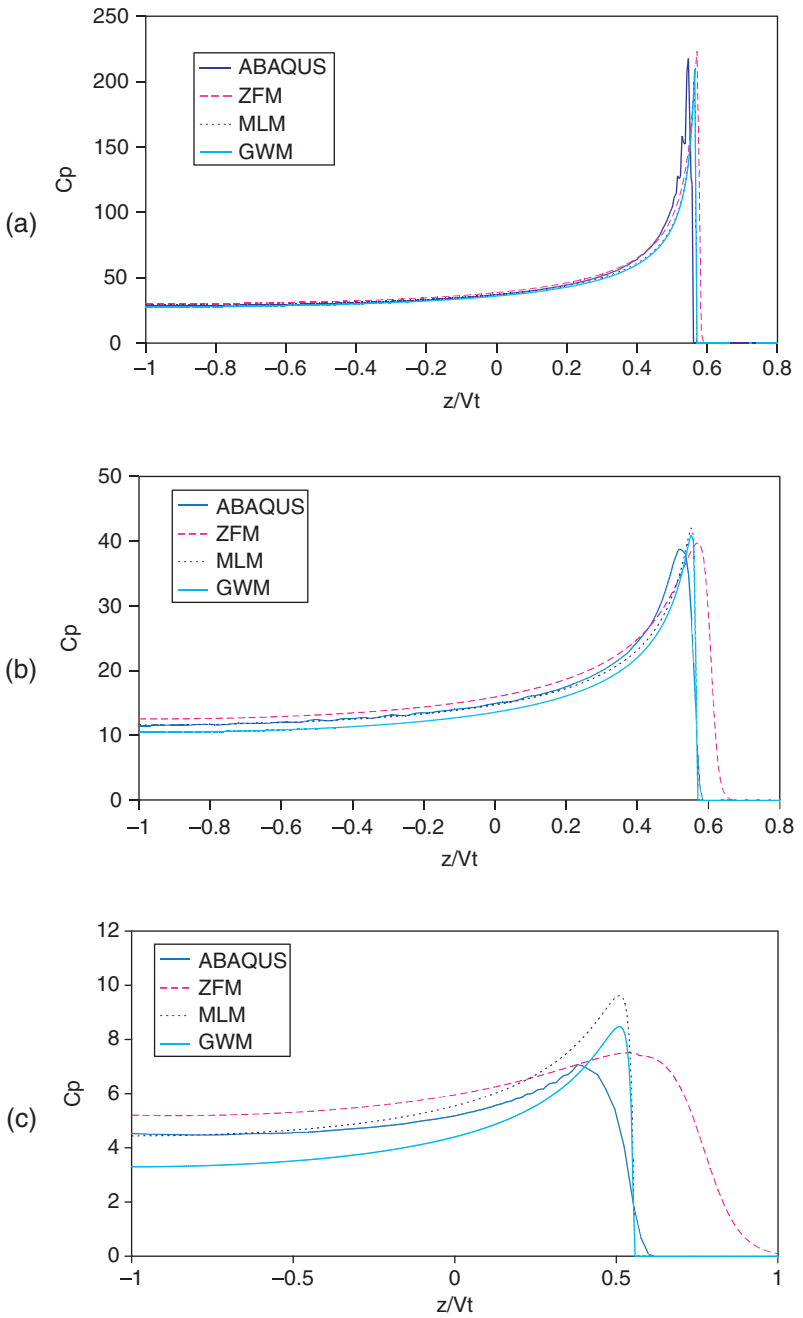


Figure 4 Distribution of pressure coefficient (eqn (23)) on a wedge entering water at constant velocity for several values of deadrise angle $\beta$. (a) $\beta = 6°$, (b) $\beta = 14°$, (c) $\beta = 30°$. $z$ is the vertical distance between the body position and the initial calm free surface.

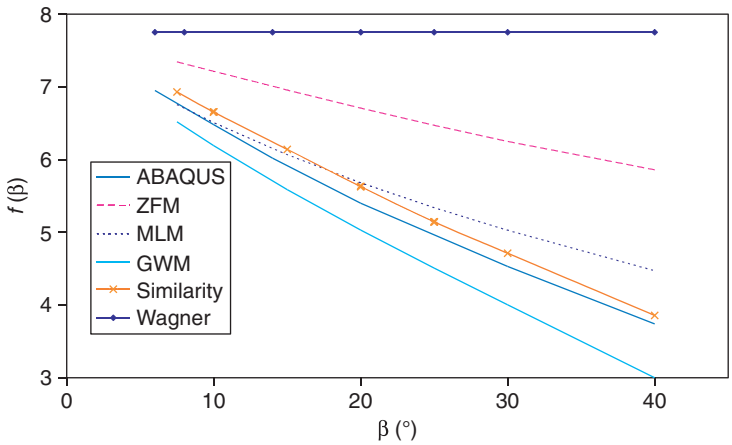


Figure 5 Force coefficient, $f(\beta) = (F \tan(\beta)^2)/(\rho L V^3 t)$, for a wedge of length $L$ entering water at constant velocity as a function of the deadrise angle $\beta$.

results of the finite element computations. As expected, the original Wagner model only provides a poor prediction of the slamming forces. The ZFM is not very much accurate. For a deadrise angle of 40°, the slamming load predicted by the ZFM is 56% greater than the results of the finite element method (or of the similarity solution). The MLM and the GWM provide better estimations of the slamming loads.

Figure 6 shows pressure distributions acting on a cone for several values of the deadrise angle. As in the 2D case, the accuracy of the analytical models decreases with the deadrise angles. However, the pressure distributions predicted by the MLM and the GWM seem to be more affected by large values of the deadrise angle than in the 2D case. In particular, the pressure near the centre of the contact surface is underestimated. The evolution of the nondimensional force acting on a cone with the deadrise angle is plotted in Figure 7. The results of experimental tests ($\beta = 7°, 15°, 30°$) carried out at ENSIETA using a hydraulic shock machine are also shown in Figure 7. More details about the experimental set-up can be found in [23]. One observes that the MLM predicts the slamming force much better than the ZFM and the GWM. For deadrise angles up to 40°, the relative difference between the results of the MLM and those of the numerical simulations are smaller than 6.2%.

## 5.2. CIRCULAR CYLINDER AND SPHERE

The impact of a circular cylinder and of a sphere of radius R at constant velocity is studied. Figure 8 presents the slamming force acting on the cylinder predicted by the analytical and numerical models, together with the experimental data of Cointe and Armand [12]. The ZFM is again shown to overpredict the slamming loads. Among the analytical models examined in the present study, the MLM seems to provide the most accurate results. Figure 9 presents the slamming load acting on the sphere. It appears that the accuracy of the GWM and the ZFM are very bad in this case. It is interesting to point out that, for a relative penetration $Vt/R$ equal to 0.1, the local deadrise angle at the intersection between the sphere surface and the liquid surface is equal to 32°. In this case, the slamming load predicted by the GWM is 32% smaller than the one obtained from the ABAQUS simulation. This discrepancy is significantly greater than the one observed for a cone with a deadrise angle of 32° (23%), see Figure 7. This indicates that the accuracy of the analytical models depends on the shape of the impacting body and not only on the maximum value of the deadrise angle.

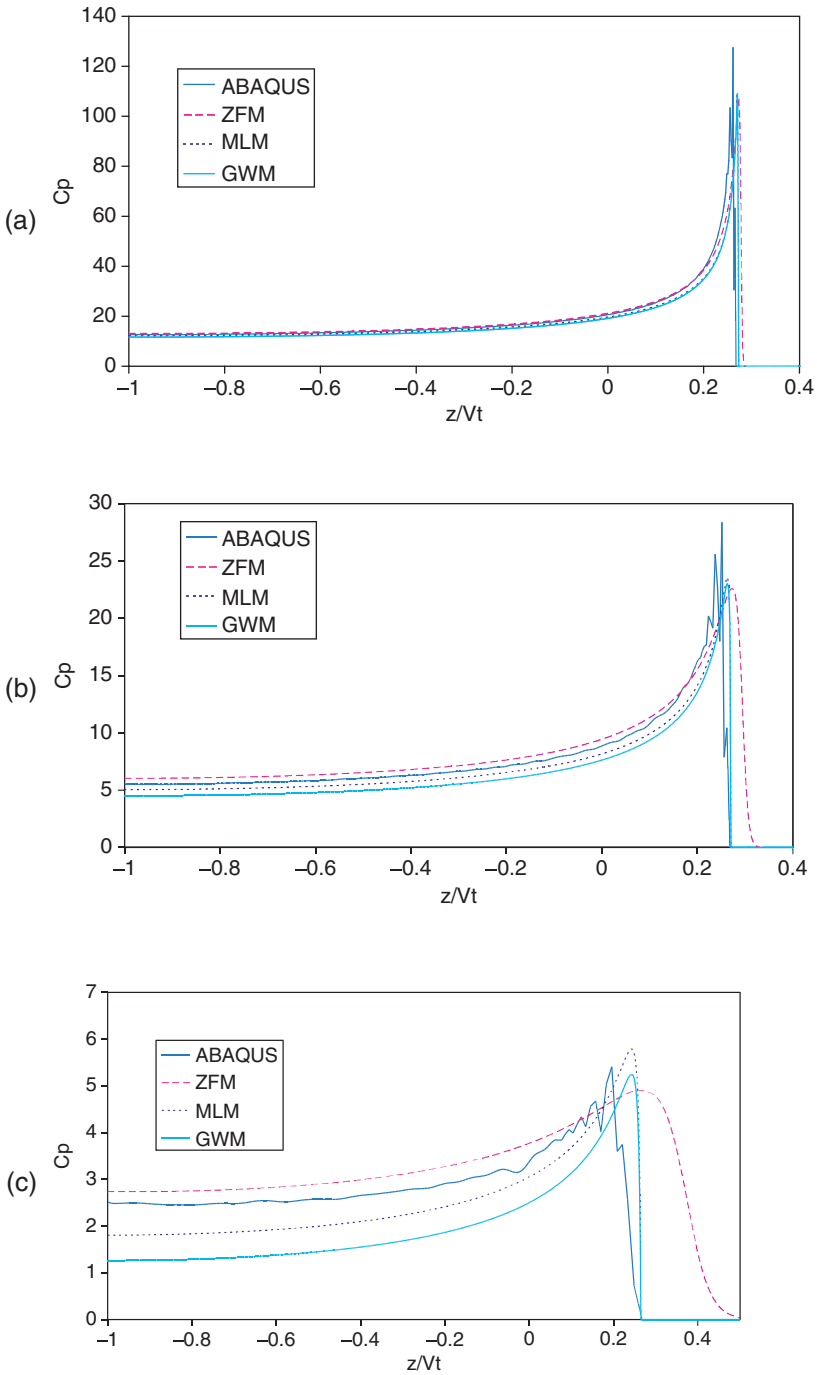


Figure 6 Distribution of pressure coefficient (eqn (23)) on a cone entering water at constant speed for several values of deadrise angle $\beta$. (a) $\beta = 7°$, (b) $\beta = 15°$, (c) $\beta = 30°$.

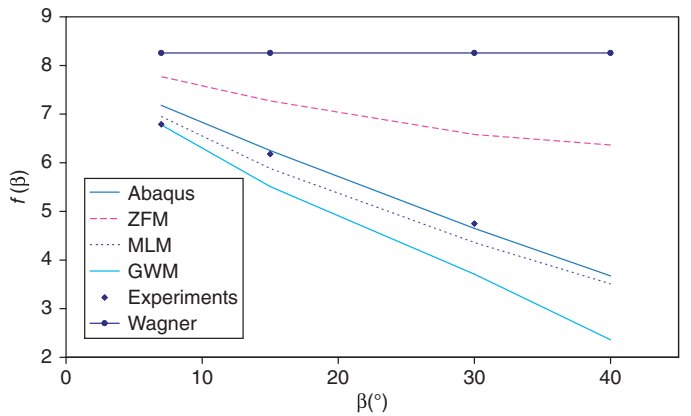


Figure 7 Force coefficient, $f(\beta) = (F \tan(\beta)^3)/(\rho V^4 t^2)$, for a cone entering water at constant velocity as a function of the deadrise angle $\beta$.

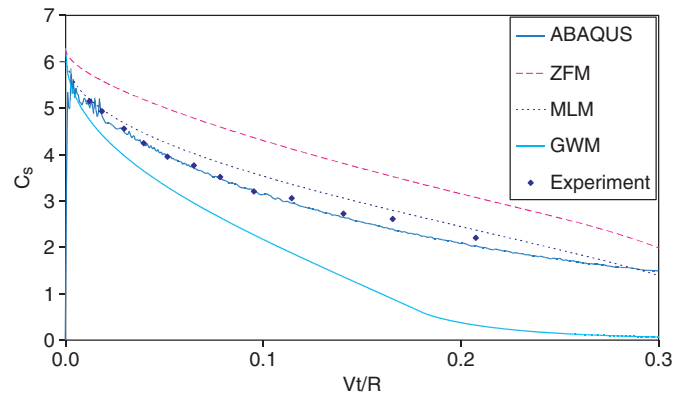


Figure 8 Nondimensional Slamming load, $C_s = F/(\rho V^2 RL)$, on a circular cylinder of radius $R$ and length $L$ as a function of the nondimensional submergence.

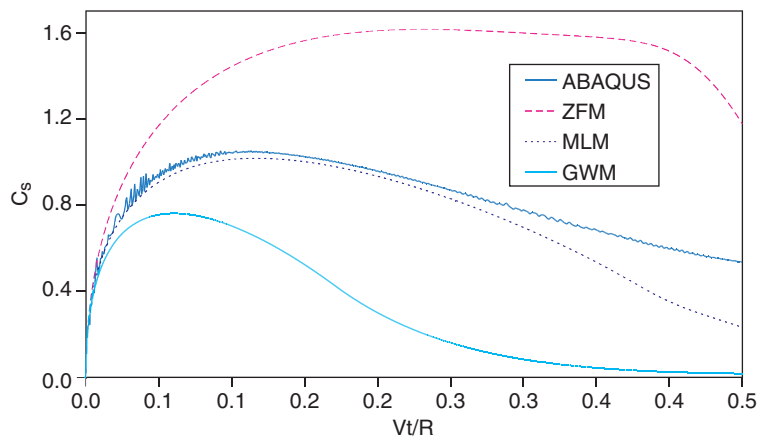


Figure 9 Nondimensional Slamming load, $C_s = 2F/(\rho V^2 \pi R^2)$, on a sphere of radius $R$ as a function of the nondimensional submergence.

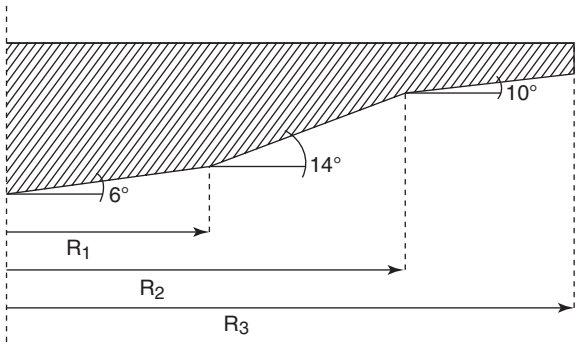


Figure 10 Axisymmetric body with knuckles ($R_1 = 90$ mm, $R_2 = 135$ mm, $R_3 = 160$ mm)

## 5.3. AXISYMMETRIC BODY WITH KNUCKLES

In this section, the impact of an axisymmetric body with sharp changes of the local deadrise angle is considered (Figure 10). Figure 11 presents the force acting on this body entering water at constant speed (12 m/s) predicted by the different models and measured during impact tests performed on the ENSIETA hydraulic shock machine. At the beginning of the impact, the load increases until the relative submergence is equal to 0.045. At this moment ($Vt/R_3 \approx 0.045$), the point of intersection between the body shape and the liquid free surface reaches the first knuckle and a rapid drop of the load is observed. It should be noticed that the analytical models predict sharper drops of the force than the finite element model and the experiments. This difference will be explained below. Then, the force increases for the second time, but at a lower rate. The change in the curves' slopes for $Vt/R_3 \approx 0.09$ corresponds to the instant when the free surface reaches the second change of deadrise angle. Figure 12 presents the distributions of pressure obtained with the MLM and a finite element simulation at three instants of time. At time $t_1$, the intersection point has not reached the first knuckle yet and the pressure distribution is similar to the pressure distribution on a cone (Figure 6.a). The fluid's compressibility is taken into account in the ABAQUS simulation. Therefore,

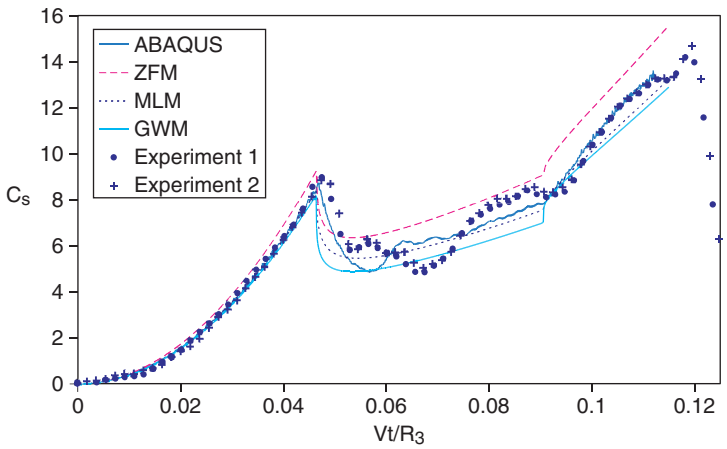


Figure 11 Nondimensional Slamming load, $C_s = 2F/(\rho V^2 \pi R_3^2)$, acting on the axisymmetric body with knuckles (Figure 10) as a function of the nondimensional submergence.

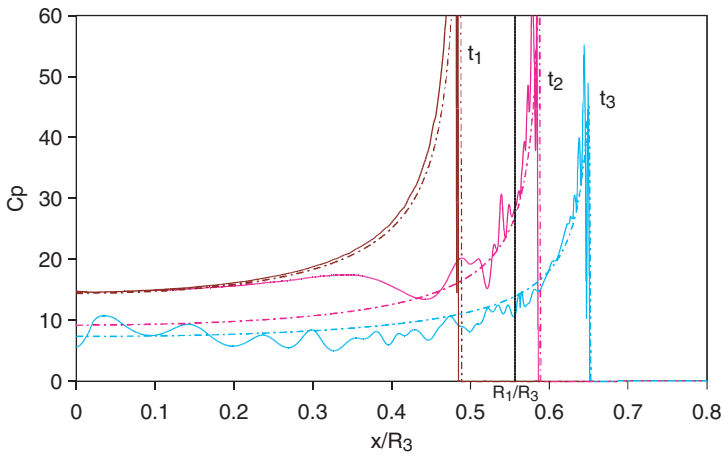


Figure 12 Distribution of pressure coefficient (Eqn. (23)) on the axisymmetric body with knuckles (Figure 10) for three different penetration depths ($Vt_1/R_3 = 4.04 \times 10^{-2}$, $Vt_2/R_3 = 4.94 \times 10^{-2}$ and $Vt_3/R_3 = 5.84 \times 10^{-2}$). Solid lines: ABAQUS, Dotted dashed lines: MLM.

when the contact surface reaches the first knuckle ($c = R_1$), a release wave is generated and propagates at finite speed toward the centre of the contact surface. That is the reason why, at time $t_2$, the pressure has dropped near the edge of the contact surface ($0.45 < x/R_3 < 0.58$), but it has not changed near the centre. Of course, such a complex phenomenon cannot be described by the MLM, which assumes that the fluid is incompressible. In that case, the hydrodynamic pressure drops rapidly on the whole contact surface when the local deadrise angle changes. That is why the MLM predicts a sharper drop of the total force after the first peak ($Vt/R_3 \approx 0.045$) than the ABAQUS simulation (Figure 11).

## 6. CONCLUSIONS

Three analytical models of water impact have been tested against results of finite element computations and experimental data. These models are based on the simplified theory of water impact introduced by Wagner [8] and make it possible to estimate pressure distributions and slamming forces without having to resort to complex numerical computations. The accuracy of these models depends on the maximum deadrise angle but also on the shape of the impacting body. Besides, this study has revealed differences between the two-dimensional and axisymmetric cases. For example, the pressure distributions obtained with the MLM and the GWM are much more affected by large values of the deadrise angle in the axisymmetric case than in the two-dimensional case. When the total hydrodynamic load is considered, the MLM is clearly more accurate than the other two models. It is, for example, the only model able to provide an estimation of the slamming load acting on a sphere consistent with the finite element simulation. An additional advantage of the MLM is that a three-dimensional version of this model is already available [24].

## REFERENCES

[1] Tuitman, J., Malenica, S., Some aspects of whipping response of container ships, *23rd International Workshop on Water Waves and Floating Bodies*. Jeju, 2008.

[2] Faltinsen, O. M., *Hydrodynamics of high-speed marine vehicles*. Cambridge University Press, New York, 2005, 286–341.

[3] Kleefsman, K. M. T., Fekken, G., Veldman, A. E. P., Iwanowski, B. and Buchner, B., A Volume-of-Fluid based simulation method for wave impact problems. *Journal of Computational Physics.* 2005, 206(1), 363–393.

[4] Aquelet, N., Souli, M. and Olovsson, L., Euler-Lagrange coupling with damping effects: Application to slamming problems, *Computer Methods in Applied Mechanics and Engineering.* 2006, 195(1–3), 110–132.

[5] Oger, G., Doring, M., Alessandrini, B. and Ferrant, P., Two-dimensional SPH simulations of wedge water entries, *Journal of Computational Physics*. 2006, 213(2), 803–822.

[6] Schellin, T. and el Moctar, O., Numerical prediction of impact-related wave loads on ships, *Journal of offshore mechanics and arctic engineering*. 2007, 129(1), 39–47.

[7] von Karman, T., The impact of seaplane floats during landing, NACA Technical note no. 321, 1929.

[8] Wagner, H., Landing of seaplanes, NACA Technical Memorandum no. 622, 1931.

[9] Chuang, S., Theoretical investigations on slamming of cone-shaped bodies, *Journal of Ship Research*. 1969, 13, 276–283.

[10] Scolan, Y.-M. and Korobkin, A. A., Three-dimensional theory of water impact. Part 1. Inverse Wagner problem, *Journal of Fluid Mechanics*. 2001, 440, 293–326.

[11] Korobkin, A. A., Analytical models of water impact, *European Journal of Applied Mathematics.* 2004, 15, 821–838.

[12] Cointe, R. and Armand, J.-L., Hydrodynamic impact analysis of a cylinder, *Journal of Offshore Mechanics and Arctic Engineering*. 1987, 109, 237–243.

[13] Zhao, R. and Faltinsen, O. M., Water entry of two-dimensional bodies, *Journal of Fluid Mechanics*. 1993, 246, 593–612.

[14] Scolan, Y.-M. and Korobkin, A. A., Energy distribution from vertical impact of a three-dimensional solid body onto the flat free surface of an ideal fluid, *Journal of Fluids and Structures*. 2003, 17, 275–286.

[15] Faltinsen, O. M., Water entry of a wedge with finite deadrise angle, *Journal of Ship Research*. 2002, 46(1), 39–51.

[16] Mei, X., Liu, Y., and Yue, D. K. P., On the water impact of general two-dimensional sections, *Applied Ocean Research*. 1999, 21, 1–15.

[17] Malleron, N., Scolan Y.-M., and Korobkin, A. A., Some aspects of a generalized Wagner model, *22nd International Workshop on Water Waves and Floating Bodies*. Plitvice, 2007.

[18] Yettou, E.-M., Desrochers, A., Champoux, Y., A new analytical model for pressure estimation of symmetrical water impact of a rigid wedge at variable velocities, *Journal of Fluids and Structures*. 2007, 23(3), 501–522.

[19] Engle, A. and Lewis, R., A comparison of hydrodynamic impacts prediction methods with two dimensional drop test data, Marine Structures. 2003, 16(2), 175–182.

[20] Scolan, Y.-M., Hydroelastic behaviour of a conical shell impacting on a quiescent-free surface of an incompressible liquid, *Journal of Sound and Vibration*. 2004, 277(1–2), 163–203.

[21] Vorus, W. S., A flat cylinder theory for vessel impact and steady planing resistance, *Journal of Ship Research*. 1996, 40(2), 89–106.

[22] Dobrovol'skaya, Z. N., On some problems of similarity flow of fluid with a free surface, *Journal of Fluid Mechanics*. 1969, 36, 805–829.

[23] Constantinescu, A., El Malki Alaoui, A., Nême, A., Rigo, P., Numerical and Experimental studies of simple geometries in slamming, *Proceedings of the 19th International Offshore and Polar Engineering Conference*. Osaka, 2009.

[24] Korobkin, A. A., Three-dimensional nonlinear theory of water impact, *Proceedings of the 18th International Congress of Mechanical Engineering*. Ouro Preto, 2005.

# Appendix: Determination of the wetted surface for arbitrary sections

In this appendix, a simple method is presented to compute the half-length of the contact surface $c(t)$ for general sections. This method is valid for both the two-dimensional and axisymmetric cases. As explained in section 2, $c(t)$ is obtained by solving the Wagner condition, eqn (6), which can be rewritten as:

$$f(c(t)) = \int_0^t U_r(c(t),\tau)d\tau \quad . \tag{A.1}$$

The relative vertical velocity $U_r$ between a particle on the free surface and the impacting body is of the form (see Eqn. (4)):

$$U_r(x,t) = V \cdot g(x, c(t)). \tag{A.2}$$

Let us introduce function $\mu$ which defines the ratio between the velocity of the impacting body and the speed of the expansion of the wetted surface:

$$\mu(c) = V\frac{dt}{dc}. \tag{A.3}$$

This function allows to rewrite the Wagner condition, Eqn. (A.1), in the following form:

$$f(c) = \int_0^c \mu(\gamma)g(c,\gamma)d\gamma. \tag{A.4}$$

Let us suppose that the range of values of interest for $c(t)$ is $[0, c_{max}]$. This interval is divided into several subintervals $[c_{k-1}, c_k]$ and over each subinterval $\mu(c)$ is assumed to be linear:

$$\mu(c) = \mu_{k-1} + \frac{c - c_{k-1}}{c_k - c_{k-1}}(\mu_k - \mu_{k-1}). \tag{A.5}$$

where $\mu_k = \mu(c_k)$. Thus, the Wagner condition becomes:

$$f(c_i) = \sum_{k=1}^{i}\left(\int_{c_{k-1}}^{c_k} \mu(\gamma)g(c_i,\gamma)d\gamma\right). \tag{A.6}$$

The integrals that appear in the right-hand side of eqn (A.6) can be calculated analytically. Therefore, the coefficient $\mu_i$ is obtained from the previous coefficients ($\mu_j$, $j$ = 0 to $i$-l) and from $f(c_i)$. $\mu_0$ is set to 0 for a flat bottom impacting body, to $2f(c_1)/(\pi c_1)$ for a two-dimensional body with an apex and to $\pi f(c_1)/(4c_1)$ for an axisymmetric body with an apex. Once the coefficients $\mu_k$ have been determined, the depths of penetration $D_i$ corresponding to each value of $c_i$ are obtained by integrating eqn (A.3):

$$D_i = D_{i-1} + \int_{c_{i-1}}^{c_i} \mu(\gamma).d\gamma = D_{i-1} + \frac{(\mu_i - \mu_{i-1})(c_i - c_{i-1})}{2} \quad \text{for } i > 0 \text{ and } D_0 = 0. \tag{A.7}$$

Thus, a table of wetted surface length values versus penetration depth is obtained. The length at a given depth is simply interpolated from this table of data.